Dynamic light scattering from lyotropic lamellar phases subjected to a flow field

A. Al Kahwaji,[1] O. Greffier,[1] A. Leon,[2] J. Rouch,[1] and H. Kellay[1]
[1]*Centre de Physique Moléculaire Optique et Hertzienne (CNRS UMR 5798), Université Bordeaux I, 341 cours de la Libération, 33405 Talence, France*
[2]*Laboratoire de Physique Statistique (UMR 8550), Ecole Normale Supérieure Paris, 24 rue Lhomond, Paris 75005, France*
(Received 31 May 2000; published 26 March 2001)

Dynamic light scattering experiments on lyotropic lamellar phases of brine and surfactant subjected to a flow field have been realized. The obtained results reveal that the relaxation times measured depend strongly on the velocity of the flow. This dependence is indicative of an increase of the effective elasticity modulus K and a decrease of the effective compressibility modulus $\overline{B}$ of the lamellar phase with the flow velocity. This leads to the conclusion that the shear can induce a suppression of the undulation fluctuations of the bilayers of the lamellar phase. Our results show also that the rigidity of the membranes decreases as the salt concentration of the sample increases.

DOI: 10.1103/PhysRevE.63.041502 PACS number(s): 62.20.Dc, 47.50.+d, 05.40.−a, 77.84.Nh

I. INTRODUCTION

The physics of complex fluids made up of surfactants in an aqueous solvent is of interest for both fundamental issues in condensed matter physics as well as for applications. Among such phases are lyotropic lamellar phases (L_α) of surfactant and brine which have attracted considerable attention from both theorists and experimentalists. These phases are composed of bilayers of surfactant parallel to each other and intercalated by water layers. They are models of systems of interacting flexible surfaces or membranes. The stability of these phases is directly related to the interactions between the bilayers which are due to electrostatic repulsions, steric forces, repulsive undulation forces, and to the elastic properties of the bilayers themselves [1,2]. The thickness of the water layer can be varied by changing the concentration of surfactant giving much control over their properties. Dilute lamellar phases can sustain different types of thermal fluctuations, namely concentration fluctuations associated with bilayer compressibility or to changes of the solvent layer thickness, and fluctuations associated with the undulations of the bilayers due to their flexibility. The hydrodynamic modes of such phases are well known both experimentally and theoretically [3,4]. From measurements of the dispersion relations of the different hydrodynamic modes of the L_α phase, the two elastic moduli characterizing this phase can be obtained. These moduli are the elasticity modulus K and the compressibility modulus B. While K is related to the bilayer flexibility, B is the product of the interactions among the bilayers. While there are a few measurements of these moduli for certain lamellar phases at equilibrium there are no measurements for L_α phases subjected to shear flow. Several recent studies have shown the extreme sensitivity of these phases to shear: these lamellar phases can be transformed into a system of monodisperse spherulites or onions at even low shears for example [5,6]. These phases also present some intriguing rheological properties as demonstrated by different studies [7–9].

Here we report a dynamic light scattering study on these microstructured soft materials, namely the lyotropic lamellar phases subjected to shear flow in flat rectangular capillaries to probe the hydrodynamics of these lamellar phases. A primary aim of this paper is to investigate the possible effects of shear flow on the hydrodynamics of lyotropic lamellar phases; in particular, we focus on the undulation and the baroclinic modes and the effect of flow on their relaxation times. Light scattering is well suited to the study of the hydrodynamics of these phases as was shown previously [4]. The scattering of light is due to both the undulation fluctuations of the bilayers and to the surfactant concentration fluctuations. One can select the observed mode by both a choice of the scattering wave vector and by controling the polarization of the light. A difficulty with such experiments stems from the fact that lamellar phases are host to a variety of topological defects; however, these defects can be annealed either by thermal treatments [4] or by shearing the solutions in capillaries [10]. The exact nature of these defects is interesting on its own and can be related to the different elastic moduli of the membranes composing the phase [11].

In dynamic light scattering experiments, depending on the scattering geometry, the measured relaxation time of the intensity autocorrelation function for oriented lamellar phases can be due to the relaxation of the undulation fluctuations (undulation mode), to the relaxation of the concentration fluctuations (baroclinic mode) or to the two fluctuation modes coupled to each other [3,4,12–18]. Following Sigaud *et al.* [16], the characteristic relaxation frequency which corresponds to the undulation fluctuations coupled to the concentration fluctuations is given by the dispersion relation

$$\omega = \frac{\overline{B} q_z^2 + K q_\perp^4}{\eta q^4 + q_z^2 \mu} q_\perp^2, \tag{1}$$

where $q_\perp$ and q_z are, respectively, the components of the wave vector q perpendicular and parallel to the direction normal to the plane of the bilayers, K is the smectic elasticity of the lamellar phase given by κ/d, where κ is the bending elastic modulus of the bilayers and d is the layer spacing. B is the compressibility modulus of the phase at constant chemical potential, η is the viscosity, and μ is a dissipative parameter and it is estimated for a large lamellar spacing d as

$d^2/12\eta$ with η the shear viscosity of the solvent [17]. In the case of a lamellar phase where it is supposed that the only dominant interaction is a long-range repulsive interaction (Helfrich interaction), there is a relation established by Helfrich [1] between κ and B,

$$\bar{B} = \frac{9\pi^2 (k_B T)^2 d}{64\kappa (d-\delta)^4}, \tag{2}$$

where δ is the thickness of the membrane, k_B is the Boltzman constant, and T is the temperature.

Now, when the wave vector is parallel to the plane of the bilayers, the only mode observed is the undulation mode and the characteristic relaxation frequency is directly related to the smectic elasticity of the lamellar phase. In this case, the dispersion relation is reduced to $\omega = (K/\eta) q_\perp^2 (3)$. In the other case where $q_\perp$ is close to zero, the characteristic frequency is due to the relaxation of the baroclinic mode and it is given by $\omega \approx \mu \bar{B} q_\perp^2 (4)$. In light scattering experiments, one can observe the baroclinic mode due to concentration fluctuations, or equivalently to the dielectric constant fluctuations in the case where the polarizations of the incident and the scattered beams are parallel. When, on the other hand, these two polarizations are crossed, the scattered intensity is sensitive to the fluctuations of the anisotropy of the dielectric constant and one can observe the undulation mode [4].

A few studies have shown the validity of this view and its relevance for measuring the elasticity and compressibility moduli of oriented lamellar phases at equilibrium [4,18–20]. In a subsequent study of the hydrodynamics of lamellar phases and the possible couplings to a hydrodynamic field, Bruinsma and Rabin [13] have shown that the expression for the dispersion relations stated above, which is applicable at equilibrium, is still valid for solutions subjected to flow in the case where the scattering vector is taken perpendicular to the flow direction. This is the case of the present study. We actually measure the dispersion relations directly in our flow cell on these phases subjected to flow and show that they are in reasonable agreement with the theoretical expressions. We then use such expressions in our data analysis to extract the effective elastic constants but it should be emphasized that flow can affect the undulations of the bilayers significantly. We assume that the effects of the flow on the undulations will be manifested as an apparent change in the elasticity and the compressibility of the phases studied. We will therefore refer to the elastic constants measured as effective constants. The variation of the effective constants measured as a function of the flow velocity is then interpreted as an effect of the flow on the fluctuations or undulations of the bilayers composing the system.

We here focus on the dependence of the relaxation time of both undulation fluctuations and concentration fluctuations of the lamellar phases on the applied shear rate and the salinity. Our findings point to the possibility that the effective smectic elasticity K of these lamellar phases increases with increasing flow velocity, indicating that flow suppresses undulation fluctuations of the bilayers. As a consequence, the effective compressibility modulus B decreases in agreement with previous results by Yamamoto and Tanaka [8]. Also, by studying these phases with variable salt concentrations we find a systematic decrease of the effective bending elasticity of the bilayers with increasing salt content in qualitative agreement with theories which predict a decrease of κ with decreasing Debye length [21–23].

II. STUDIED SYSTEMS

In this present study we have used two different systems. The first one is composed of pure water, an ionic surfactant AOT (bis-ethylhexyl-sulfosuccinate sodium salt), and varying amounts of salt (NaCl). The phase diagram of this system was extensively studied by Gosh and Miller [24]. At a constant concentration of ionic surfactant and for variable concentrations of salt, this phase diagram shows a transition from a sponge phase to a lamellar phase and to a phase of spherulites. The phase of spherulites is presumably metastable although some recent work tends to support the idea that these phases are equilibrium phases [25]. Let us first briefly describe the phase diagram obtained at a temperature of 22 °C for a concentration of 7% of surfactant in water (by weight) and for salt concentrations ranging from 0% to 3% by weight. At high salt concentrations (above 1.75%) a sponge phase or L_3 phase is obtained. This phase occupies the whole volume of the tube; it is an optically isotropic bluish phase of low viscosity. The structure of this disordered phase is bicontinuous with a surfactant bilayer separating the solvent into two interconnected and continuous regions [26,27]. At higher salt concentrations this phase rejects water and becomes more viscous and its volume decreases. At low salt concentrations below the one-phase L_3 region, a coexistence region between L_3 and L_α phases is seen between 1.475% and 1.75% salt. The volume of the lamellar phase increases as the salt concentration decreases. Below 1.475% a one-phase lamellar region is observed; the lamellar spacing for this surfactant concentration is about 40 nm. The lamellar phases are birefringent and therefore easily distinguished from the L_3 phases which are isotropic. As the salinity decreases the lamellar phase becomes slightly more turbid. At salt concentrations below 0.9% a phase of spherulites is obtained: these are liquid-crystalline particles constituted of several concentric bilayers separated by water.

The second system we have studied is composed of a nonionic surfactant ($C_{12}E_5$: penta-ethyleneglycol mono *n*-dodecyl ether), a cosurfactant (hexanol), and pure water. At a cosurfactant to surfactant mass ratio of 0.27 in a solution of pure water containing a 0.3% mass fraction of hexanol, a lamellar phase is obtained for an interval of cosurfactant and surfactant concentration varying between 1% and 10% volume fraction. One can then obtain a lamellar phase with lamellar spacing varying from a few hundred to a few thousand angstroms [28]. In our study we have used a lamellar phase with a lamellar spacing of 3300 Å. The lamellar spacing was estimated as $d = \delta/\phi$ where δ is the bilayer thickness (33 Å for the $C_{12}E_5$) and ϕ is the volume fraction of cosurfactant and surfactant [18,28]. Due to the very dilute nature of this lamellar phase, the defects are difficult to visualize.

There are marked differences between the two systems studied. These differences stem from the dilute nature of the $C_{12}E_5$ lamellar phase used compared to the lamellar phases based on the AOT surfactant. The $C_{12}E_5$ lamellar phase has shown experimentally a viscosity of 2 mPa s and is Newtonian in the sense that the shear viscosity is independent of the shear rate in the range between 4 and 200 s^{-1}. Measurements at lower shear rates than 4 s^{-1} were difficult to carry out and showed quite a bit of noise. The AOT lamellar phases used are more concentrated and have a lamellar spacing about an order of magnitude smaller than the nonionic lamellar phase. The AOT phases have viscosities which are much higher than the solvent viscosity (water) and show marked shear thinning behavior. The viscosity of all the AOT lamellar phases used depends strongly on the shear rate and decreases as the shear rate increases. The AOT lamellar phases have been shown in previous studies of their rheology to present some peculiar features. A bistability was found for presheared samples of these phases [7]. Also, if these phases are sheared at a constant shear rate for long periods of time, a very large increase of the viscosity has been observed [6]. This increase is associated with the formation of onionlike objects in the lamellar phase.

We stress these differences here since as it turns out, the viscosity of the lamellar phase needs to be taken into account in the analysis of the data. The dilute $C_{12}E_5$ lamellar phase which is of low viscosity and Newtonian (for shear rates above 4 s^{-1} which is roughly the range used here) serves as a test system where the rheology is simple. In addition, this latter system has already been characterized by dynamic light scattering (the method we use here) albeit at equilibrium, and allows us to compare our data with the results of such studies.

III. EXPERIMENTAL SETUP

The dynamic light scattering measurements are carried out using an argon laser ($\lambda = 514.3$ nm) operating at a power between about 100 and 300 mW, a photomultiplier to collect the scattered light, and a logarithmic correlator (ALV5000). In order to produce flow we have used flat capillaries (from Hellma) with a length of 3 cm, a width of 1 cm and a gap size of 0.1 cm. The liquid was pumped with a motorized syringe that guarantees a constant volumetric flow rate of the liquid. This volumetric flow rate can be varied from 0.2 to 5 cm^3/min. In this paper we will refer to a velocity rather than to a volumetric flow rate; this velocity is the mean velocity of the flow calculated from the volumetric flow rate divided by the cell section. The fluid was injected into the capillary through a 0.4-cm-diam plastic flexible tube; the diameter of this tube was chosen to be larger than the gap of the flat capillary to minimize the effect of shearing the solution in the tube. The length of this tube had no effect on the measured autocorrelation functions. The capillaries used are of good optical quality and because they are flat allowed us to choose a scattering wave vector parallel or oblique to the membranes once the lamellar phase is oriented with its bilayers parallel to the cell walls. The geometry of our optical set up is horizontal while the cell was oriented vertically. In this way the flow was in the vertical direction allowing us to avoid the effect of Doppler shift. The scattering vector was perpendicular to the velocity vector and it could be chosen parallel or perpendicular to the cell walls (see Fig. 1 for optical arrangement).

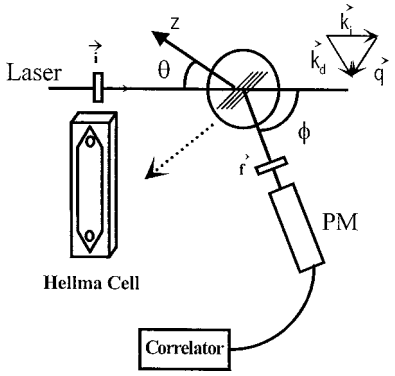

FIG. 1. Optical arrangement for dynamic light scattering measurements. The cell is oriented vertically while the optical plane is horizontal. The scattering wave vector q is perpendicular to the velocity vector. When $\phi = 2\theta$, $q_z = 0$, and the wave vector is parallel to the cell walls.

The intensity autocorrelation functions were measured in two different optical configurations. In the first one, we measure the autocorrelation function with an incident beam polarized vertically and an analyzer in front of the photomultiplier oriented horizontally (VH configuration). In this configuration and in the case where the lamellars are oriented parallel to the cell walls, the correlation time measured for scattering wave vectors taken parallel to the cell walls (scattering wave vectors in the plane of the layers with the component parallel to the layer normal being very close to zero) is due to the undulation fluctuations [4]. For this case the cell is actually slightly tilted with respect to the vertical direction to ensure coupling to anisotropic dielectric constant fluctuations.

In the second configuration the polarization of the incident beam and the analyzer are both oriented vertically (VV configuration). This last configuration allows us to measure the relaxation time of the baroclinic mode in the case where the component of the scattering wave vector in the plane of the layers becomes small compared to that perpendicular to the membranes [4].

IV. EXPERIMENTAL RESULTS

Let us now describe the results we have obtained in the two different optical configurations (VH and VV) corresponding to the undulation mode and to the baroclinic mode, respectively.

A. Undulation mode

1. Autocorrelation functions

As can be seen in Fig. 2 for a lamellar sample at 1.4 wt % salt concentration, the shape of the obtained autocorrelation function in the VH configuration depends on the flow veloc-

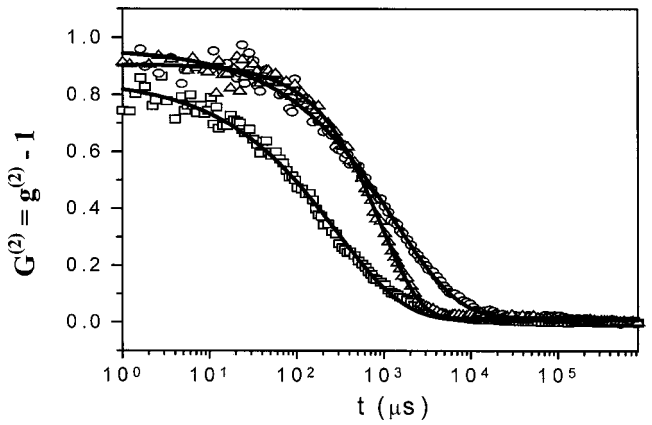

FIG. 2. Autocorrelation functions $G^{(2)}(t)=g^{(2)}(t)-1$ for a lamellar phase at 1.4 wt % salt concentration in the VH configuration for different flow velocities. Squares are for an equilibrated phase. Circles and triangles are for flow velocities of 0.83 and 2.5 mm/s, respectively. The autocorrelation function is a stretched exponential at equilibrium with a stretching exponent of 0.56, this stretching exponent increases with the velocity and reaches values close to 1 for flow velocities greater or equal to a velocity we call $V_{\max}$. The stretching exponent is 0.6 for 0.83 and 0.97 for 2.5 mm/s.

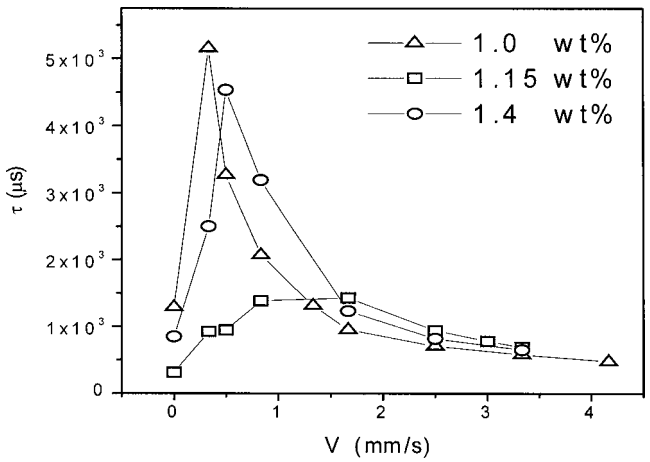

FIG. 3. Relaxation time as a function of the flow velocity for different salt concentrations in the VH configuration. Squares, circles, and triangles correspond, respectively, to 1.4, 1.15, and 1 wt % salt concentrations. Note that the flow velocity $V_{\max}$ corresponding to the maximum of the relaxation time increases with salt concentration.

ity. This function is a stretched exponential at rest and at low velocities with a stretching exponent around 0.65. At higher velocities, the stretching exponent increases and reaches values close to 1 near a certain velocity that we call $V_{\max}$. At velocities above $V_{\max}$, the autocorrelation function is a single exponential. This indicates that the lamellar phase at rest or flowing at small velocities is full of defects and therefore the lamellae have different orientations in the scattering volume, and that the flow helps orient the lamellar phase as shown by the single exponential behavior at higher flow rates. This observation is in agreement with previous results on the effect of shear flow on L_α phases [10]. This is confirmed by visual observations of the phases in polarized microscopy where defects are seen below $V_{\max}$ and the solution becomes dark with few defects at velocities above $V_{\max}$. Defects are, however, observed near the lateral boundaries of the cell. As we will see below, the velocity $V_{\max}$ depends on the salinity of the phase and increases with the salt concentration. Similar behavior for the shape of the autocorrelation function was observed for the lamellar phase of the $C_{12}E_5$/hexanol/water system. Here again, the obtained autocorrelation function is a stretched exponential at rest and at low velocities with a stretching exponent around 0.7. The stretching exponent increases then with the velocity to reach values close to 1 near a certain velocity $V_{\max}$. At velocities above $V_{\max}$, the autocorrelation function obtained is a single exponential. Again, flow helps to orient the lamellar phase. As stated earlier, however, the defects are more difficult to visualize in this system as it is very dilute.

2. Characteristic relaxation time

A typical dependence of the relaxation time on the flow velocity at $q_z=0$ ($\phi=\pi/2$ and $\theta=\phi/2$) and in VH configuration is shown for the AOT lamellar phases at different salt concentrations within the one-phase lamellar region and for the $C_{12}E_5$ lamellar phase in Figs. 3 and 4, respectively. The behavior observed is relatively similar in the two cases: the characteristic time first increases, reaches a maximum at a well-defined velocity ($V_{\max}$), and decreases as the flow velocity increases. As stated above $V_{\max}$ corresponds to the velocity for which the autocorrelation function of the scattered light becomes a single exponential. Note that the velocity $V_{\max}$ corresponding to the maximum of the characteristic relaxation time increases with the salinity. As the salt concentration increases, the position of the peak shifts to higher flow rates, indicating that for the higher salt concentrations the transition to an oriented state occurs at higher velocities. This shift in the position of the peak may be related to the proximity of the sponge phase which is the equilibrium phase at higher salinities. It is probable that the na-

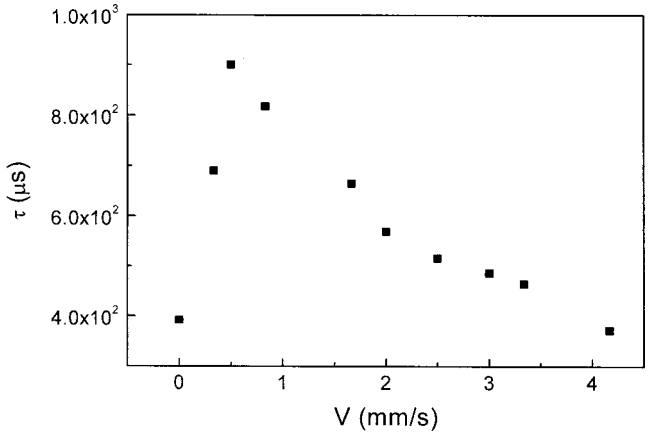

FIG. 4. Relaxation time as a function of the flow velocity for a $C_{12}E_5$/hexanol/water lamellar phase at 0.27 hexanol/$C_{12}E_5$ mass ratio and 1% volume fraction of surfactant and cosurfactant (lamellar spacing of 3300 Å).

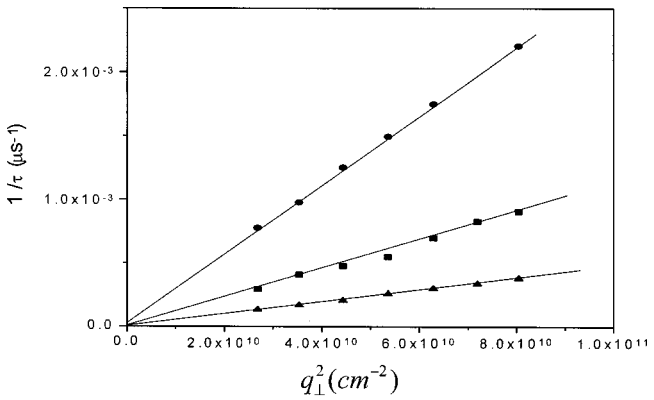

FIG. 5. Inverse of the relaxation time $1/\tau$ as a function of $q_\perp^2$ for a lamellar phase at 1.0 wt % salt concentration in the VH configuration for different flow velocities above $V_{\max}$. Circles, squares, and triangles are, respectively, for 1.67, 0.83, and 0.50 mm/s flow velocities.

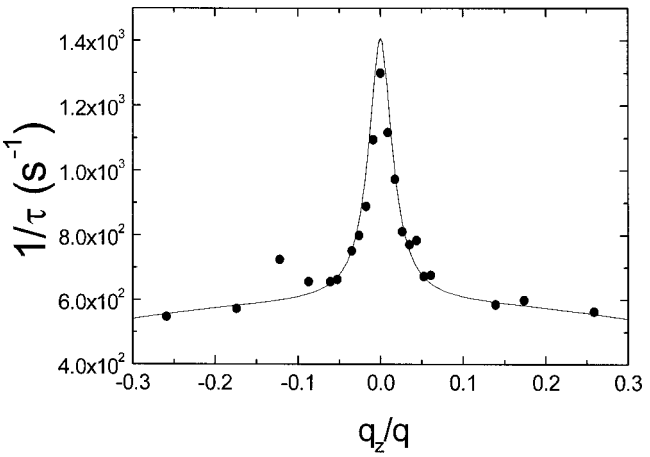

FIG. 6. Relaxation frequency in VH configuration near $q_z=0$ as a function of q_z/q. The dispersion relation of the undulation and/or baroclinic mode is well verified. The peak frequency corresponds to the undulation mode and allows us to estimate the value of κ. The experimental plot is for an AOT lamellar sample at 1.15% salt concentration and for a flow of 1.66 mm/sec. The theoretical fit gives a value of $4.3\times10^{-12}\,\mathrm{m^2\,s^{-1}}$ for K/η.

ture of the defects present in the lamellar phase as well as their change upon approaching the sponge phase affect how the lamellar phase orients with the flow. Another manifestation of the effects of salt, as we will show below, is that the elasticity of the bilayers decreases as the salinity increases and therefore as the sponge phase is approached. Also the decrease of the relaxation time with the flow velocity observed after $V_{\max}$ is not as important for the higher salinities. This decrease of the characteristic time with the velocity is more pronounced for the low salinity AOT phases than for the $C_{12}E_5$ lamellar phases as well. The decrease of the correlation time above $V_{\max}$ will be interpreted below and related in part to an increase of the effective bending elasticity of the membranes with an increasing velocity. The increase of the correlation time between the no-flow situation ($V=0$) and the velocity $V_{\max}$ is, on the other hand, more difficult to interpret. The main reason for this is the absence of a single exponential for the autocorrelation function of the scattered light. The relaxation times of the autocorrelation function can be related to the viscous and elastic response only when the autocorrelation function is a single exponential. There is no direct predictions for the nonexponential case for which the presence of defects complicates the hydrodynamics. One may only speculate at the present time about such an increase.

Let us now describe the dependence on the scattering wave vector of the measured characteristic frequency (inverse of the characteristic time: $1/\tau$) at $q_z\approx0$ for the VH configuration. Here we will only be concerned with flow velocities above $V_{\max}$ since the theoretical dispersion relations apply only to oriented lamellar phases for which the autocorrelation functions are necessarily exponential. In Fig. 5 we plot the relaxation frequency (at $q_z\approx0$ and for the VH configuration) as a function of $q_\perp^2$ for an AOT lamellar sample of 1 wt % salt concentration and for different velocities above $V_{\max}$. Note that the higher the velocity, the smaller the decay time is for all q values studied. The fact that the measured characteristic frequency is linear in $q_\perp^2$ is in agreement with the dispersion relation of the undulation mode of the lamellar phase which was stated above. An additional test showing this agreement comes from Fig. 6 where we present the VH relaxation frequency measured near $q_z=0$ and for a flow velocity above $V_{\max}$ as a function of q_z/q. Figure 6 shows that the dispersion relation (1) is well verified and that the characteristic frequency presents a peak at $q_z=0$ ($\phi=2\theta$). The peak frequency allows us to estimate the bending elasticity κ. Figure 6 was obtained for a lamellar phase sample at 1.1 wt % salt concentration and for a flow velocity of 1.66 mm/sec. We will return later to the values of the physical parameters used for this fit. As it turns out this fit is sensitive to the ratio K/η but not very sensitive to the value of B.

B. Baroclinic mode

1. Autocorrelation functions

The observed VV autocorrelation functions present the same behavior as those observed in the VH configuration: A stretched exponential at low velocities with a stretching exponent around 0.65. The stretching exponent increases then with the velocity to reach values close to one for velocities equal or larger than $V_{\max}$.

2. Characteristic relaxation time

To observe the characteristic relaxation time of the baroclinic mode, we follow the same procedure as in Ref. [4]. For a flow velocity above the velocity $V_{\max}$ we measure the relaxation time in VV configuration for different fixed values of the wave vector q with scans in q_z and $q_\perp$ for each q value. The scan in q_z and $q_\perp$ is obtained by varying the angle θ between the cell normal and the incident beam (see Fig. 1). The q value is fixed by the scattering angle ϕ. The relaxation frequencies in VV configuration as a function of $q_\perp^2$ for a lamellar sample of 1.3 wt % salinity and for a flow velocity

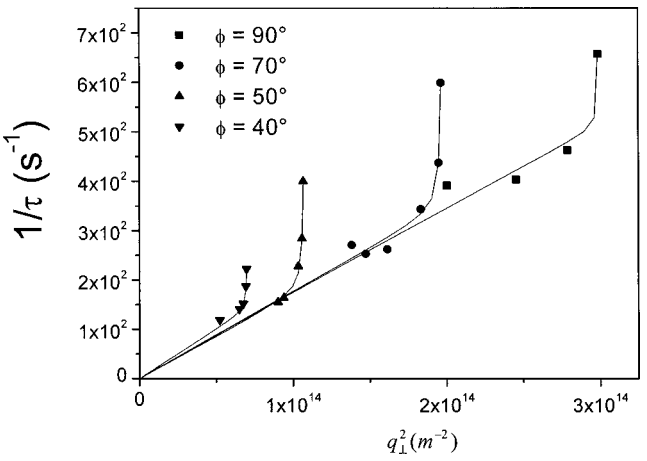

FIG. 7. Relaxation frequency in VV configuration as a function of $q_\perp^2$ for an AOT lamellar sample of 1.3 wt % salinity and for a flow velocity of 2.5 mm/s. The different results are obtained by fixing the value of the wave vector q and doing a scan in q_z and $q_\perp$. The solid lines are the theoretical fits obtained by the general dispersion relation. The fits give about $2\times10^4\ s^{-1}$ and about $10^{-12}\ m^2\ s^{-1}$ for B/η and K/η, respectively.

of 2.5 mm/s is shown in Fig. 7. The results in Fig. 7 are reasonably well fit by the general dispersion relation (1) and one can estimate the value of the compressibility parameter B. Note that the relaxation frequency increases for q_z close to zero and it is linear in $q_\perp^2$ far from $q_z=0$. In the latter case, the corresponding relaxation frequency can be approximated by $\omega\sim\mu B q_\perp^2$(4) as was stated above. Figure 8 shows the characteristic relaxation frequency in the VV configuration far from $q_z=0$ for the 1.3 wt % salt concentration lamellar phase at two different flow velocities (1.66 and 2.5 mm/s). Note that the observed relaxation frequency dependence seems to be linear in $q_\perp^2$.

V. DISCUSSION

Let us now comment on the dependence of the relaxation time as a function of velocity. First, as specified earlier, the

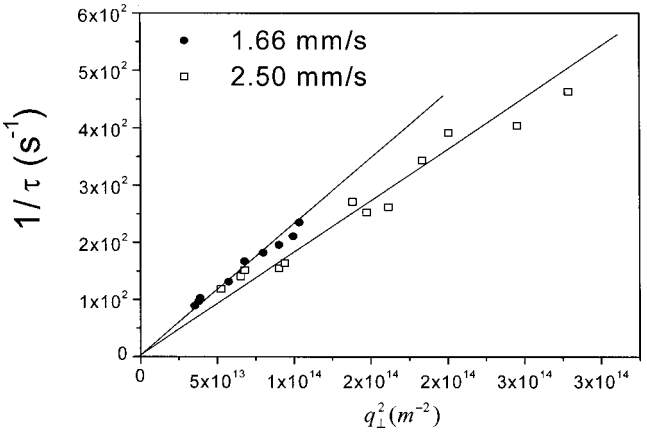

FIG. 8. Relaxation frequency in VV configuration as a function of $q_\perp^2$ far from $q_z=0$ for an AOT lamellar sample of 1.3 wt % salinity and for two different flow velocities. Squares and circles are, respectively, for 1.66 and 2.5 mm/s.

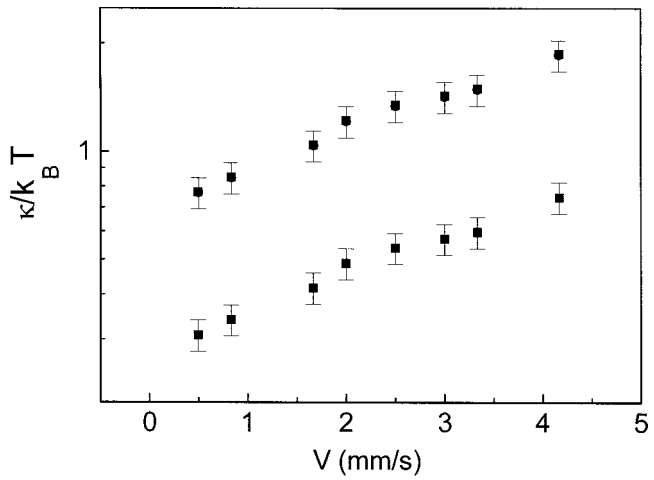

FIG. 9. Bending elastic modulus κ as a function of the flow velocity for the $C_{12}E_5$ lamellar phase at 3300 Å lamellar spacing. These values were extracted from the measured undulation relaxation times using either the viscosity of the solvent (lower curve) or the viscosity of the phase (upper curve). Note that the values obtained for κ are more important when using the viscosity of the phase but the variation versus the velocity remains the same.

scattering vector is taken perpendicular to the flow direction, therefore the time measured cannot be due to a Doppler shift. Recall that the Doppler shift introduces a relaxation time given by $(\mathbf{V}\cdot\mathbf{q})^{-1}$. The dependence we find is quadratic in the scattering vector which was set perpendicular to the velocity direction and which should not couple to the velocity. Second, different salt concentrations give different decay times for the same velocity, again indicating that the measured times are not due to a Doppler shift. Also, similar experiments performed on L_3 phases show that the measured correlation time depends little on the velocity of the flow for these phases in contrast to the lamellar phases. For similar reasons the decay time we measure is not due to a transit time of inhomogeneities going through the scattering volume.

Furthermore, many studies have shown that for an oriented lamellar phase and when the scattering wave vector is in the plane of the layers, the measured VH relaxation time is due to the undulation mode [3,4]. Then, the correlation time we measure at $q_z=0$ in the VH configuration for velocities above V_{max} can be attributed to the relaxation of the undulation fluctuations of the bilayers of the lamellar phase. This is in agreement with the fact that the VH measured characteristic frequency is linear in $q_\perp^2$ and that the dependence of this frequency on q_z/q near $q_z=0$ can be well fit by the general dispersion relation (Fig. 6). On the other hand, the mode observed at $q_z q_\perp\neq0$ far from $q_z=0$ corresponds to the baroclinic mode (as verified by a test of the dispersion relation for this mode) and the corresponding relaxation frequency allows us to estimate the compressibility modulus B of the phase [4,18].

Let us now try to estimate the effective bending elastic modulus κ and the effective compressibility modulus B of the lamellar phases used and their dependence on the flow velocity. Figure 9 shows the dependence of the bending elas-

tic modulus κ on the flow velocity for the $C_{12}E_5$ lamellar phase with a lamellar spacing of 3300 Å. The κ values were extracted from the measured relaxation frequency of the undulation mode using Eq. (3) and taking the viscosity of the interstitial solvent (water, $\eta = 1$ mPa s in our case). Note that the bending elasticity tends to increase with the velocity and the obtained κ values vary between $0.3k_BT$ and $0.75k_BT$, which is in rough agreement with the values obtained at equilibrium for the same system [18,19]. On the other hand, the estimation in the same way of the effective bending elastic modulus κ for the AOT lamellar samples leads to κ values which are too small compared to the thermal energy $k_BT(0.005-0.05k_BT)$. Moreover, the results would indicate a very large, and difficult to explain, increase of κ with the flow velocity. If we now extract the effective compressibility modulus B from the measured relaxation frequency of the baroclinic mode using expression (4) and taking the viscosity of the interstitial fluid (water), once again we find very small values for the AOT lamellar phases compared with what was obtained in [18,19] for a $C_{12}E_5$ lamellar phase of a comparable lamellar spacing. The values obtained for a lamellar phase of 1.3 wt% salt concentration are 28 and 22 Pa for, respectively, 1.66 and 2.5 mm/s. All this leads to the conclusion that there should be another parameter to consider in addition to the bending elasticity and to the compressibility of the phase. This additional parameter could be the viscosity. In fact, many dynamic light scattering studies on concentrated colloidal suspensions have proposed the use of the viscosity of the sample at zero shear rate [29]. We must stress here that the use of a zero shear rate viscosity for lyotropic lamellar phases is problematic since defects are present in such solutions at rest. As we show below the relevant viscosity to use in our case is the shear viscosity of the phase as well as its dependence on the shear rate used. For the sake of completeness we extracted the zero shear rate viscosity by extrapolation to the zero shear rate and used them in the dispersion relations measured. The values of the bending elastic modulus κ we obtain from the undulation relaxation frequency are more reasonable, $(0.7-1.5)k_BT$ for the $C_{12}E_5$ lamellar phase (Fig. 9 upper curve) and of the order of k_BT for the AOT samples. However, the increase of the rigidity κ with the flow velocity for the AOT phases remains very difficult to explain. κ increases by approximately a factor 10 in this case. Using the viscosity of the phase at zero shear leads to more reasonable values of the compressibility modulus B as well (for example, we obtain for a 1.3 wt% salt concentration AOT lamellar phase, B values of 5056 and 3926 Pa for, respectively, 1.66 and 2.5 mm/s). These values are, however, an order of magnitude larger than the values found in [18,19].

The other possibility now is to use the shear viscosity of the lamellar phase. In the study of the hydrodynamics of the lamellar phase, it is the viscosity of the solvent which was usually considered [4,17]. However, Bruinsma and Rabin [13] who have studied the effect of shear flow on the lamellar phase have considered a surfactant concentration-dependent viscosity. The dependence of the measured undulation and baroclinic relaxation frequencies on the flow velocity may be due to the variation of the viscosity with the shear rate as flow can introduce local variations of the surfactant concentration. What we suggest to do here is to estimate the bending elasticity using the viscosity of the phase measured at the corresponding velocities or shear rates in the dispersion relation of the undulation mode [Eq. (3)]. For the $C_{12}E_5$ lamellar phase at 3300 Å, the dependence of the rigidity κ on the flow velocity remains the same because this sample is Newtonian in the range of shear rates studied here (above 4 s^{-1} which corresponds roughly to V_{max} for this system) and its viscosity does not vary with the shear rate.

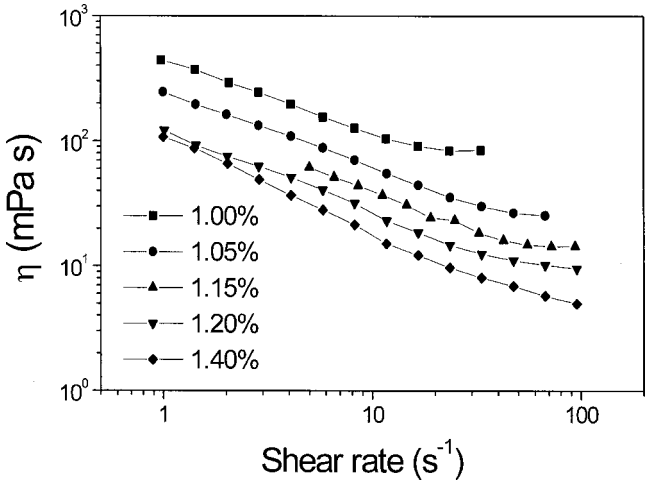

FIG. 10. Shear viscosity η as a function of the shear rate γ for samples in the lamellar region and for different salt concentrations as indicated in the figure. The viscosity decreases considerably with the shear rate. For a fixed shear rate, the viscosity decreases with the salinity.

The situation is quite different for the AOT system, measurements of the shear viscosity as a function of the shear rate realized on the lamellar phases of this system (using a Couette geometry with a gap of 1 mm on a Stress Tech rheometer from Reologica Instruments) show a strong dependence of the viscosity on the shear rate. Viscosity as a function of the shear rate for samples of different salinities in the lamellar region are shown in Fig. 10. Note that the viscosity of these samples is considerably higher than the viscosity of the solvent (water). As the shear rate increases the viscosity decreases considerably. The viscosity also decreases with salinity for a fixed shear rate. As a note of caution, let us stress that the viscosity of the solution depends on the history of the sample. If the sample is sheared at a constant shear rate for long periods of time (10–20 min) the viscosity shows a large increase as time elapses and the solution becomes gel-like with viscosities of order 1 Pa s [7]. Our measurements were carried out on fresh samples that were left at rest for periods of a few hours before the measurements; in addition to that we subject the sample to small shear rates and for times much shorter than the time for which a viscosity increase is observed. This experimental protocol was followed for the correlation measurements as well to minimize the sensitivity to the history of the sample. The dependence of the measured undulation relaxation frequency on the flow velocity can then be interpreted by an increase of the rigidity of the bilayers but also by a decrease

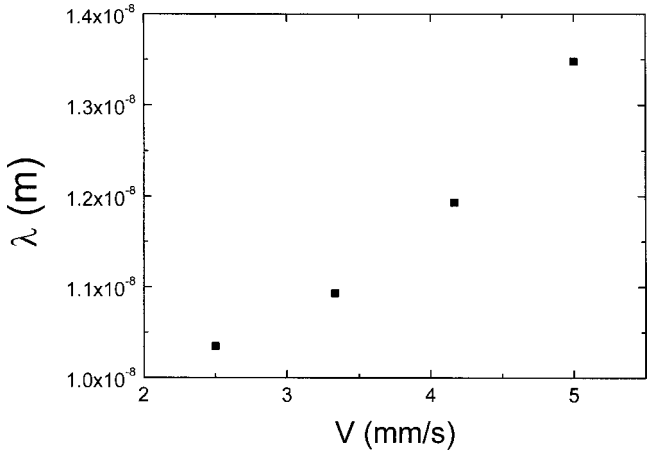

FIG. 11. Penetration length λ as a function of the flow velocity for an AOT lamellar sample of 1.25 wt % salinity. Note that λ increases with the velocity indicating the suppression of undulation fluctuations of the bilayers of the phase.

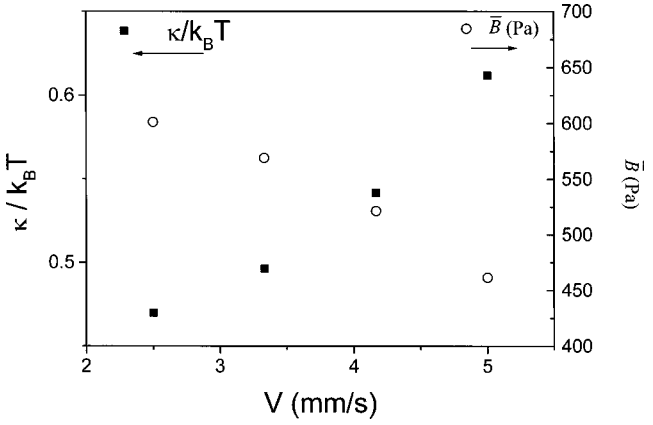

FIG. 12. The bending elastic modulus κ and the compressibility modulus B as a function of the flow velocity for an AOT lamellar sample of 1.25 wt % salinity.

of the viscosity of the phase. However, because of the difficulty in determining the velocity profile in the cell and consequently the shear rate and the corresponding viscosity to use, the estimation of the bending elasticity is still difficult to do especially for the AOT lamellar phases.

This problem could be solved, as we will see, by measuring for the same sample, both the relaxation frequency of the VH mode at $q_z=0$ (undulation mode) and that of the VV mode at $q_z q_\perp \neq 0$ with $q_z \gg q_\perp$ (baroclinic mode). We then estimate K/η and B/η separately for the same sample. One can then estimate the penetration length $\lambda=\sqrt{K/B}$ [30]. Using the Helfrich relation between κ and B [Eq. (2)], we can now estimate the rigidity κ and the compressibility B of the phase without supposing any condition on the viscosity. Despite the fact the membranes are charged in our case, the salt addition reduces the Debye length and the Helfrich steric interaction dominates over the repulsive electrostatic interactions. The thickness of the membrane δ is about 21 Å in our case [28].

To test this proposition, we measured the two relaxation frequencies (undulation mode and baroclinic mode) as shown before for a lamellar phase at 7 wt % AOT and 1.25 wt % salt concentration and for different flow velocities above $V_{\max}$. We then estimated the variation of the penetration length λ with the velocity using the K/η and B/η values extracted from the measured undulation and baroclinic relaxation frequencies. Figure 11 shows the dependence of the penetration length λ on the velocity for the 1.25 wt % salt concentration lamellar phase. Note that the penetration length increases with the flow velocity. This can indicate an increase of the bending elasticity, a decrease of the compressibility modulus, or the two together. The increase of the penetration length with the flow velocity is indicative of a suppression of undulation fluctuations of the bilayers. Using the Helfrich relation (2), we can obtain the variation of κ as a function of the flow velocity as shown in Fig. 12 for the 1.25 wt % salt concentration lamellar phase (we can also obtain the B values which are inversely proportional to κ [Eq. (2)]). This result shows that the effective elasticity of the lamellar phase increases (while the compressibility modulus decreases) as the flow velocity increases. This is indicative of the suppression of undulation fluctuations of the bilayers composing the phase. Furthermore, we can estimate the variation of the viscosity as a function of the flow velocity using the K/η and κ or the B/η and B values. Comparing the obtained values for the viscosity with the measured viscosity values using a rheometer (Fig. 10), we can also have an estimate of the average shear rate in the cell. The result we obtain is that the shear rate is given by $\approx 5.5V/b$ (V is the mean flow velocity and b is the cell gap) which is slightly higher than $3V/b$ obtained supposing a Poiseuille profile. The shear rates found fall in the range 3 to 50 s^{-1}.

Once the average shear rate in the cell is estimated, we can extract the variation of the bending elasticity directly from the characteristic relaxation frequency of the undulation mode using the corresponding viscosity measured experimentally. Figure 13 shows the dependence of the estimated effective elasticity on the flow velocity obtained for different salt concentrations. The trends we noted is an increase of κ as a function of velocity and a decrease as a function of salt concentration. The increase of the bending elasticity is important for low salinities, but becomes less important as the salinity increases. For the lamellar sample of 1 wt % salt concentration, κ increases by roughly a factor of 2 as the speed increases. The increase of the effective elastic bending modulus with the velocity has not been observed before and the effect is indicative of a suppression of undulation fluctuations of the bilayers. However, the decrease of the compressibility modulus with the shear indicative also of the suppression of undulation fluctuations has been observed before by Yamamoto and Tanaka [8]. Although the fact that κ decreases with increasing salt concentration is in qualitative agreement with theories [21–23], this prediction could not explain the large variation we find. Our study puts forth the possibility that both the ionic strength of the solution and the flow velocity affect the bending elasticity modulus of the bilayers and therefore the smectic elasticity of the lyotropic lamellar phases. Our findings can have significant consequences on understanding the effects of hydrodynamic flow on such complex phases.

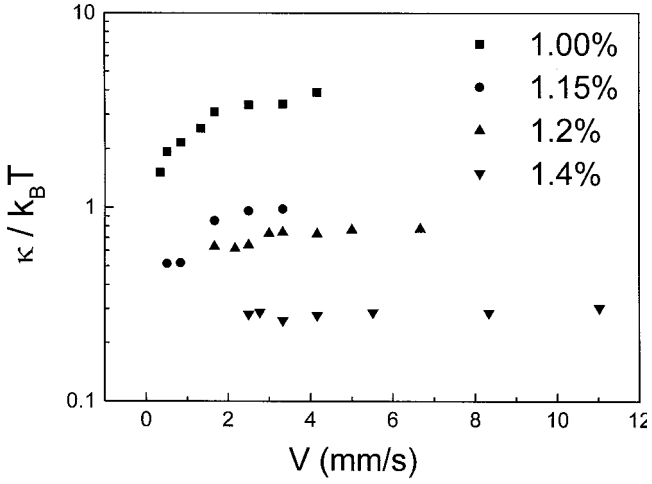

FIG. 13. Bending elastic modulus κ as a function of the flow velocity for different salt concentrations. Squares, circles, up triangles, and down triangles are, respectively, for 1, 1.15, 1.2, and 1.4 wt %. These values were extracted from the measured relaxation times and using the viscosity of the phase measured at the corresponding shear rate.

VI. CONCLUSION

We report on a study of the dynamics of lyotropic lamellar phases undergoing shear flow. Our findings point out that the lamellar phases can be oriented by shear flow as was found previously [10] allowing us to deduce the values of the effective bending elastic modulus of the bilayers composing the phases as well as the effective compressibility modulus of the lamellar phase. We use dynamic light scattering and a formalism introduced in Ref. [4] to relate the decay time of the undulation fluctuations as well as the concentration fluctuations of the lamellar phase to the bending elasticity of the bilayers and to the compressibility of the phase. We find that the effective bending elasticity modulus depends on the salt content of the lamellar phase which has been predicted theoretically. Also this modulus depends on the velocity of the flow as this modulus increases as the flow velocity increases pointing to the possibility that flow suppresses undulation fluctuations in lyotropic lamellar phases. As a consequence of this supression, the effective compressibility modulus decreases in agreement with previous observations. The shear flow suppresses the fluctuations in these systems giving rise to an enhanced apparent elasticity and a reduced apparent compressibility.

ACKNOWLEDGMENTS

This work was partially supported by a grant from Le Conseil Régional d'Acquitaine as well as a grant from MENRT. We are very grateful to J. Meunier and D. Bonn for much help in carrying out the viscosity measurements as well as for fruitful discussions. We would like to thank F. Nallet for a critical reading of the manuscript as well as for several suggestions concerning the experiments.

[1] W. Helfrich, Z. Naturforsch. A **33**, 305 (1978).
[2] D. Sornette and N. Ostrowsky, in *Micelles, Membranes, Microemulsions and Monolayers*, edited by W. M. Gelbart, A. Ben-Shaul, and D. Roux (Springer-Verlag, New York, 1994), p. 251.
[3] F. Nallet, D. Roux, and J. Prost, Phys. Rev. Lett. **62**, 276 (1989).
[4] F. Nallet, D. Roux, and J. Prost, J. Phys. II **50**, 3147 (1989).
[5] O. Diat and D. Roux, J. Phys. II **3**, 9 (1993).
[6] A. Léon, D. Bonn, J. Meunier, A. Alkahwaji, O. Greffier, and H. Kellay, Phys. Rev. Lett. **84**, 1335 (2000).
[7] D. Bonn, J. Meunier, O. Greffier, A. Al kahwaji, and H. Kellay, Phys. Rev. E **81**, 18 (1998); **58**, 2115 (1998).
[8] J. Yamamoto and H. Tanaka, Phys. Rev. Lett. **74**, 932 (1995).
[9] D. Roux, F. Nallet, and O. Diat, Europhys. Lett. **24**, 53 (1993).
[10] D. Roux and C. M. Knobler, Phys. Rev. Lett. **60**, 373 (1988).
[11] P. Boltenhagen, O. Lavrentovich, and M. Kleman, J. Phys. II **1**, 1233 (1991).
[12] P. C. Martin, O. Parodi, and P. S. Pershan, Phys. Rev. A **6**, 2401 (1972).
[13] R. Bruinsma and Y. Rabin, Phys. Rev. A **45**, 994 (1992).
[14] R. Messager, P. Bassereau, and G. Porte, J. Phys. II **51**, 1329 (1991).
[15] D. Roux, C. R. Safinya, and F. Nallet, in *Micelles, Membranes, Microemulsions and Monolayers* (Ref. [2]), p. 303.
[16] G. Sigaud, C. W. Garland, H. T. Nguyen, D. Roux, and S. T. Milner, J. Phys. II **3**, 1343 (1993).
[17] F. Brochard and P. G. de Gennes, Pramana Suppl. 1, 1 (1975).
[18] E. Freyssingeas, D. Roux, and F. Nallet, J. Phys. II **7**, 913 (1997).
[19] E. Freyssingeas, Thesis of University of Bordeaux I, 1994.
[20] A. Ott, W. Urbach, D. Langevin, R. Ober, and M. Waks, Europhys. Lett. **12**, 395 (1990).
[21] M. Winterhalter and W. Helfrich, J. Phys. Chem. **92**, 6865 (1988).
[22] H. N. W. Lekkerkerker, Physica A **159**, 319 (1989).
[23] D. J. Mitchell and B. W. Ninham, Langmuir **5**, 1121 (1989).
[24] O. Gosh and C. A. Miller, J. Phys. Chem. **91**, 4528 (1987).
[25] E. van der Linden and C. J. Buytenhek, Physica A **245**, 1 (1997).
[26] D. Roux, C. Coulon, and M. E. Cates, J. Phys. Chem. **96**, 4174 (1992).
[27] G. Porte, M. Delsanti, I. Billard, M. Skouri, J. Appell, J. Marignan, and F. Debeauvais, J. Phys. II **1**, 1101 (1991).
[28] M. Skouri, J. Marignan, J. Appell, and G. Porte, J. Phys. II **1**, 1121 (1991).
[29] A. Imhof, A. Van Blaaderen, G. Maret, J. Mellema, and J. K. G. Dhont, J. Chem. Phys. **100**, 2170 (1994).
[30] P. G. de Gennes, J. Phys. Suppl. **30**, C4-65 (1969).